Electronic Supplementary Material (ESI) for Lab on a Chip.

Supplementary Information for

Silicon chambers for enhanced incubation and imaging of microfluidic droplets

Nicolas Lobato-Dauzier[1,2‡], Robin Deteix[1,2‡], Guillaume Gines[3], Alexandre Baccouche[1,2], Benediktus Nixon Hapsianto[2], Shu Okumura[1,2], Guilhem Mariette[1,2], Djaffar Belharet[4], Samuel Lequeste[4], Laurent Jalabert[1,2], Matthieu Denoual[5], Yannick Rondelez[3], Hiroshi Toshiyoshi[1,2], Hiroyuki Fujita[6], Soo Hyeon Kim[1,2], Teruo Fujii[1,2], Anthony J. Genot[1,2*]

1 LIMMS, CNRS-Institute of Industrial Science, IRL 2820, The University of Tokyo, Tokyo 153-8505, Japan

2 Institute of Industrial Science, The University of Tokyo, Meguro, Tokyo 153-8505, Japan

3 Laboratoire Gulliver, CNRS UMR 7083, ESPCI Paris, PSL Research University, Paris 75005, France

4 Institut FEMTO-ST, Université Bourgogne Franche-Comté, CNRS UMR 6174, Besançon 25030 , France

5 GREYC, CNRS UMR 6072, ENSICAEN, Caen 14000, France

6 Advanced Research Laboratories, Tokyo City University, Setagaya, Tokyo 158-0082 , Japan

‡ These authors contributed equally to this work

* Author to whom correspondence should be addressed

Email: genot@iis.u-tokyo.ac.jp

Additional Figures and Tables

Properties	PDMS	Silicon
Mechanical stiffness (Young modulus) (Pa)	3.6-8.7 $\cdot 10^{5}$ [1]	1.30 $\cdot 10^{11}$ [2]
Thermal conductivity (W $m^{-1}K^{-1}$)	0.15 [3]	130 [4]
Coefficient of thermal expansion α ($°K^{-1}$)	200-300 $\cdot 10^{-6}$ [5]	2.6 $\cdot 10^{-6}$ [6]
Reflectance (%)	5-10 [7]	40-80 [8]

Table S1 Comparison of some mechanical, thermal and optical properties of PDMS and silicon.

Chambers nominal depth	Measured depth at center	Measured depth at border	Measured depth max variation
50 µm (N=15)	49.5 ± 1.7 µm	52.2 ± 2.3 µm	3.5 ± 1.1 µm
10 µm (N=15)	9.6 ± 0.2 µm	10.1 ± 0.3 µm	0.6 ± 0.2 µm

Table S2 Characterization of the depth of the silicon chambers for the 6-inch wafer process. Typical distance from center to border is 5 mm

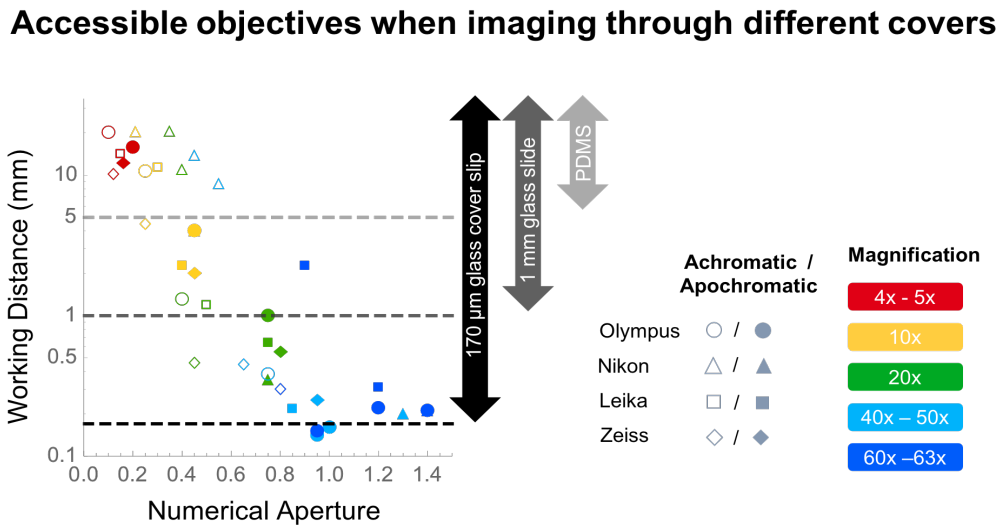

Figure S1. Numerical Aperture and Working distance of typical microscope objectives. The objectives with the best performances (Apochromatic with a large Numerical Aperture) are only accessible when using a 170 µm glass cover slip due to their shorter Working Distances. A slab of PDMS is typically a few millimeters thick, and the glass slides used to bond with PDMS are usually ~1 mm thick

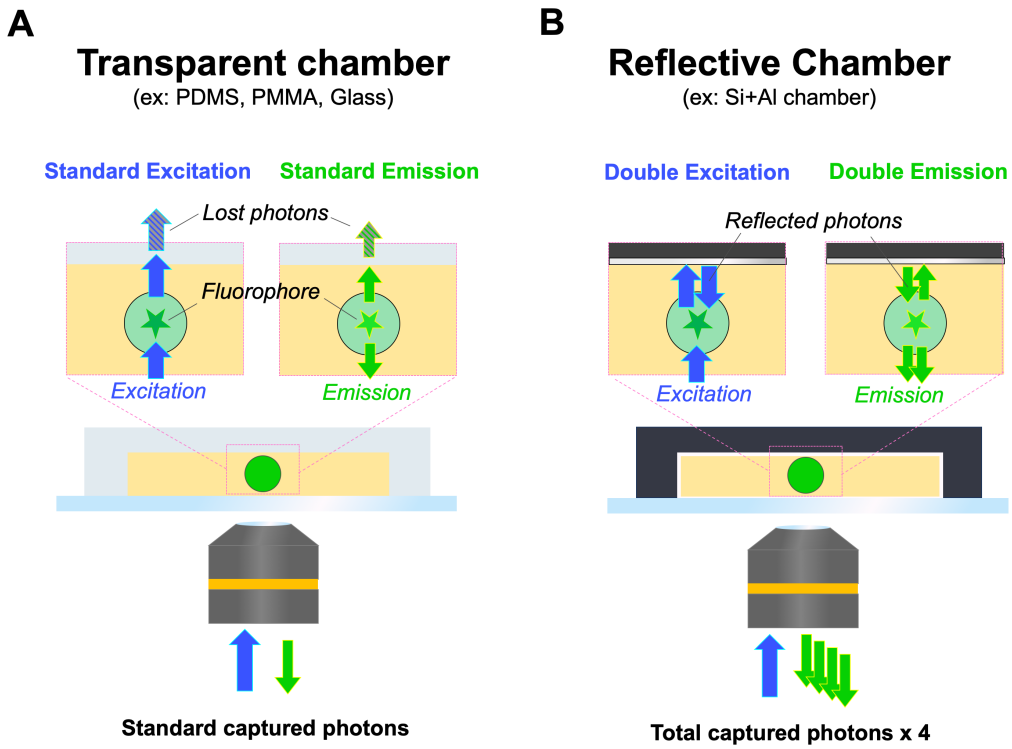

Figure S2. Effect of chamber reflectivity on total captured photons. A, Standard fluorescence imaging using a transparent chamber. Only a portion of emitted photons can be collected, the others being lost at the back. **B**, Effect of having a reflective chamber on excitation and fluorescence emission. Excitation light is reflected at the back of the chamber effectively doubling the excitation. Similarly, emitted photons are also reflected. Considering a full reflection, the total captured photons can be enhanced by a factor of 4.

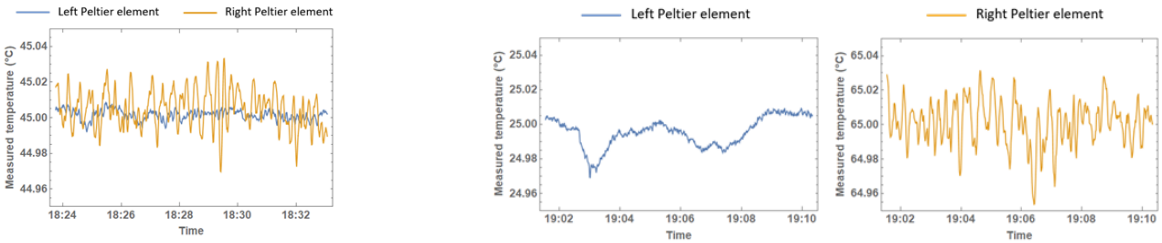

Figure S3. Temperature stability of the Peltier setup in uniform (left) or gradient (right) mode. The right Peltier element is noisier because being often used for heating 40°C above the room temperature which requires higher currents than on the left side.

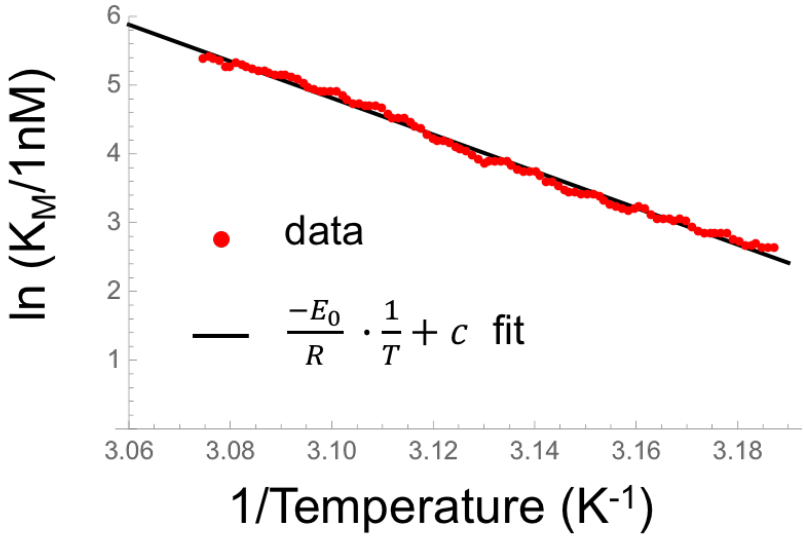

Figure S4. Linear Fit of natural logarithm of K_M against the inverse of the temperature. This linear dependence shows that $K_M \propto e^{\frac{-E_0}{RT}}$ with $E_0 = 2.2 \cdot 10^5\, J$.

Nucleic acid sequences

Name	Sequence
Let-7a-RNA	UGA GGU AGU AGG UUG UAU AGU U
alpha: Bo12	CATTCATCCCAG
aT: CBo12-2PS3	C*T*G*GGATGAATGCTGGGATGAA
pT: pTBoT5S3P	T*T*T*TTCTGGGATGAATG
rT: rTBo-2BsmIAtto633	Atto633*C*T*TCATGAATGCTGGGATGAAG BHQ2
Let7atoBo-2+2P	TGCTGGGATGAAGTTTGACTCAAACTATACAACCTACTACCTCA

Table S3. DNA and RNA sequences for the multiplexed digital assay (Figure 2). * denotes a phosphorothioate backbone

Name	Sequence
Beacon Bottom: Cd11bex8 bottom	ATTACGAATTCACCAATGACGTAGCGAATGACTCCTAT-Atto647N
Beacon Top: Cd11bex8 top	BBQ 650-ATAGGAGTCATTCGCTACGTCATTGGTGAATTCGTAAT

Table S4. High temperature molecular beacon (Figure 3 B)

Name	Sequence
Clamp Switch	Atto 488-ATTTTCTTTTCCCCCCAGTTATTATTCCCCCCTTTTCTTTTG-BHQ1
Stab 12	AAAAGAAAAGGG
Stab 11	AAAAGAAAAGG
Stab 10	AAAAGAAAAG
Stab 9	AAAAGAAAA

Table S5. DNA nanothermometers[9] sequences used in Figure 3 C,D

Name	Sequence
input α: X2	CATTCACGATAG
output β: Ba12	CATTCTGACGAG
cT: X2 to Ba12	C*T*C*GTCAGAATGCTATCGTGAATG
rt: MB.Ba12 HEX	HEX-*T*T*CTGA TTTTCTCGTCAGAA-BHQ1

Table S6. DNA sequences used for the thermal mapping of Michaelis-Menten constants. * denotes a phosphorothioate backbone

Solutions contents

Optical enhancement & Photobleaching	
Component	Concentration
Additional mQ water	70 %
NEB 3.1 buffer (10x)	1x
dextran FITC	100 nM
dextran Rhodamine	0 / 100 nM
dextran alexa 647	100 / 0 nM

1X NEB 3.1 buffer (pH=7.9 @25°C)	
Component	Concentration
NaCl	100 mM
Tris-HCl	50 mM
MgCl2	10 mM
BSA	100 µg/ml

Table S7. Composition of the droplets used for the optical characterization of the chamber (Figure 1 D,E)

Multiplexed digital assay	
Component	Concentration
mir Buffer	25 µM
Let 7a	0 / 8 / 40 / 200 / 1000 / 5000 fM
dextran Texas Red	0 / 0 / 400 / 0 / 200 / 200 nM
dextran Cascade blue	0 / 400 / 0 / 200 / 200 / 0 nM
dextran Alexa 488	400 / 0 / 0 / 200 / 0 / 200 nM
aT: CBo12-2PS4	50 nM
pT: pTBo12T5SP	12 nM
cT: Let7atoBo-2+2P	0.5 nM
rT: MB.Bo-2Bsm1Cy5	40 nM
BSA9000S	200 µg/mL
Nb.BsmI	300 u/mL
Vent(exo-)	70 u/mL
BsmI	7 u/mL
ttRecJ	13 nM
ntBstNBI	10 u/mL
in CFX96 @50°C	

mir Buffer	
Component	Concentration
NaCl	100 mM
Tris-HCl	50 nM
MgCl2	10 nM
BSA	100 µg/ml

Table S8. Composition of the droplets used for the multiplexed isothermal assay (Figure 2)

Droplets tracking with heating	
Component	Concentration
Additional mQ water	76%
Clamp buffer	0.25 x
BSA9000S	200 µg/mL
Beacon Top	500 nM
Beacon Bottom	500 nM
EvaGreen	1x
Dextran Cascade Blue	100 nM
Dextran Alexa 555	0 / 100 nM

Clamp buffer (pH=7)	
Component	Concentration
HEPES	50 mM
NaCl	300 mM
MgCl2	10 mM

Table S9. Composition of the droplets used for the characterization of the chamber at high temperatures (Figures 3 B & Figure 1 C)

Silicon chamber temperature calibration using DNA nanotermometers	
Component	Concentration
Additional miliQ water	61 %
Clamp buffer	1x
BSA9000S	200 µg/mL
dextran Alexa 555	100 nM
Clamp Switch atto 488-BHQ	100 nM
Stab 9	400 / 0 / 0 / 0 nM
Stab 10	0 / 400 / 0 / 0 nM
Stab 11	0 / 0 / 400 / 0 nM
Stab 12	0 / 0 / 0 / 400 nM
dextran Cascade Blue	0 / 0 / 100 / 100 nM
dextran Alexa 647	0 / 100 / 0 / 100 nM

Table S10. Composition of the droplets used for the characterization of the thermal gradient Figure 3 C,D

***En masse* thermal mapping of Michaelis-Menten constants**	
Component	Concentration
Additional miliQ water	55%
Smix buffer	1x
dNTP	400 µM
rt: MB.Ba12 HEX	200 nM
cT: X2toBa12	10 nM
dextran Cascade Blue	200 nM
BSA9000S	200 µg/mL
Nb.BsmI	450 u/mL
Vent (exo-)	70 u/mL
input α: X2	0 to 200 nM
Dextran Alexa 647	0 to 200 nM

Table S11. Composition of the droplets used for the mapping of Michaelis-Menten constants presented in Figure 4

Mathematical estimate of thermal loss

Let us consider a simplified model of heat losses: a material of thickness *L* has one of its sides in contact with a heater at temperature 60°C, and the other side in contact with air (with a temperature of 22°C far from the material). The material transfers heat to the environment (i.e. the air side) by convection and radiation. We assume that the material is thin and that the temperature of the side exposed to air is close to 60°C. The convective heat rate with air is given by Newton's law and we assume that the heat transfer coefficient is independent of the material and fixed by the surrounding air medium, for which we take a heat transfer coefficient of 10 W m^{-2} K^{-1} (typical for free convection). Then the material loses ~380 W m^{-2} by convection to air. It also loses 224 W m^{-2} by radiative transfer according to the Stefan–Boltzmann law (assuming an emissivity of 0.95). These heat losses are compensated by the establishment of a temperature gradient in the bulk of the material; the more thermally conductive the material is, the less the temperature drops. The differential of temperature ΔT between the hot and cold side of the material is $k/L\Delta T=P_{loss}$, where L is the thickness and k the thermal conduction. For glass, the temperature drop is ΔT=0.75 °C over a thickness of 1 mm, while the drop is negligible for silicon (less than 4 mK).

References

[1] D. Armani, C. Liu, and N. Aluru, “Re-configurable fluid circuits by PDMS elastomer micromachining,” 1999, pp. 222–227.

[2] J. Wortman and R. Evans, “Young’s modulus, shear modulus, and Poisson’s ratio in silicon and germanium,” *Journal of applied physics*, vol. 36, no. 1, pp. 153–156, 1965.

[3] A. C. Kuo, “Poly (dimethylsiloxane),” *Polymer data handbook*, pp. 411–435, 1999.

[4] C. J. Glassbrenner and G. A. Slack, “Thermal conductivity of silicon and germanium from 3 K to the melting point,” *Physical Review*, vol. 134, no. 4A, p. A1058, 1964.

[5] A. Müller, M. C. Wapler, and U. Wallrabe, “A quick and accurate method to determine the Poisson’s ratio and the coefficient of thermal expansion of PDMS,” *Soft Matter*, vol. 15, no. 4, pp. 779–784, 2019.

[6] Y. Okada and Y. Tokumaru, “Precise determination of lattice parameter and thermal expansion coefficient of silicon between 300 and 1500 K,” *Journal of applied physics*, vol. 56, no. 2, pp. 314–320, 1984.

[7] A. Zahid, B. Dai, R. Hong, and D. Zhang, “Optical properties study of silicone polymer PDMS substrate surfaces modified by plasma treatment,” *Materials Research Express*, vol. 4, no. 10, p. 105301, 2017.

[8] M. A. Green and M. J. Keevers, “Optical properties of intrinsic silicon at 300 K,” *Progress in Photovoltaics: Research and applications*, vol. 3, no. 3, pp. 189–192, 1995.

[9] D. Gareau, A. Desrosiers, and A. Vallée-Bélisle, “Programmable quantitative DNA nanothermometers,” *Nano letters*, vol. 16, no. 7, pp. 3976–3981, 2016.